Table 4
The effect of chronic adrenomedullin infusion on the levels of proteinuria during feeding on the high sodium diet in DS rats in protocol 2

| Urinary protein (mg/day/100gBW) | 2nd-week | 3rd-week | 4th-week |
|---|---|---|---|
| DR-S | 3.4±1.1 | 3.2±0.9 | 3.4±0.9 |
| DS-S | 5.2±1.7* | 6.5±2.5** | 7.8±2.7** |
| DS-AM | 3.5±1.0[b] | 4.5±1.2[b] | 5.7±1.6[a] |

[a] $p<0.05$ vs DS-S.
[b] $p<0.01$ vs DS-S.
* $p<0.01$ vs DR-S.
** $p<0.0001$ vs DR-S.

and cortical and medullary nNOS expression, and 4) adrenomedullin may stimulate renal nNOS level in the macula densa and inner medullary collecting duct. These results suggest that chronic adrenomedullin infusion has beneficial effects on this hypertension probably in part through increased eNOS expression in renal medulla and nNOS expression in macula densa and inner medullary collecting duct in DS rats and that renal adrenomedullin may serve as an endogenous protective mechanism against salt-sensitive hypertension.

Adrenomedullin infusion has been reported not only to reduce systemic blood pressure in spontaneously hypertensive rats [13] and healthy human subjects [14], but also to increase urinary sodium excretion in anesthetized normal dogs [15]. These results suggested that adrenomedullin may regulate systemic blood pressure and urinary sodium excretion. However, the involvement of adrenomedullin has not been reported in the reduction of urinary sodium excretion that causes salt-sensitive hypertension in Dahl rats. Since we showed that the increased level of renal adrenomedullin correlated both with systemic blood pressure and urinary sodium excretion, there is a possibility that renal adrenomedullin is involved in the modulation of salt-sensitive hypertension in DS rats. Furthermore, chronic adrenomedullin infusion attenuated the increase of blood pressure and heart weight, suggesting that increased renal adrenomedullin may serve as an endogenous protective mechanism against salt-sensitive hypertension.

NO has been shown to play an important role in various physiological processes in the kidney, including sodium and fluid reabsorption [16], renal hemodynamics [17] and tubuloglomerular feedback [18]. Endogenous NO is enzymatically produced from the conversion of the amino acid L-arginine to L-citrulline, a reaction that is catalyzed by NOS. Three different NOS isoforms have been identified; namely a nNOS, a eNOS, and an inducible (iNOS) isoform, which are differentially expressed throughout the kidney [19]. Previous report demonstrated that renal eNOS activity was comparable between DS and DR rats under the high sodium diet [5]. We also compared the expression of eNOS protein in renal medulla and cortex, respectively between DS and DR rats. In the renal cortex eNOS expression had no significant difference between DS and DR rats after the 3-week high sodium diet. It was almost a similar result with the above report [5]. However, in the renal medulla eNOS expression was significantly reduced in DS rats compared with DR rats. Taken together with the fact that the inhibition of NOS causes salt-sensitive hypertension, the reduced eNOS expression in the renal medulla may be involved in part

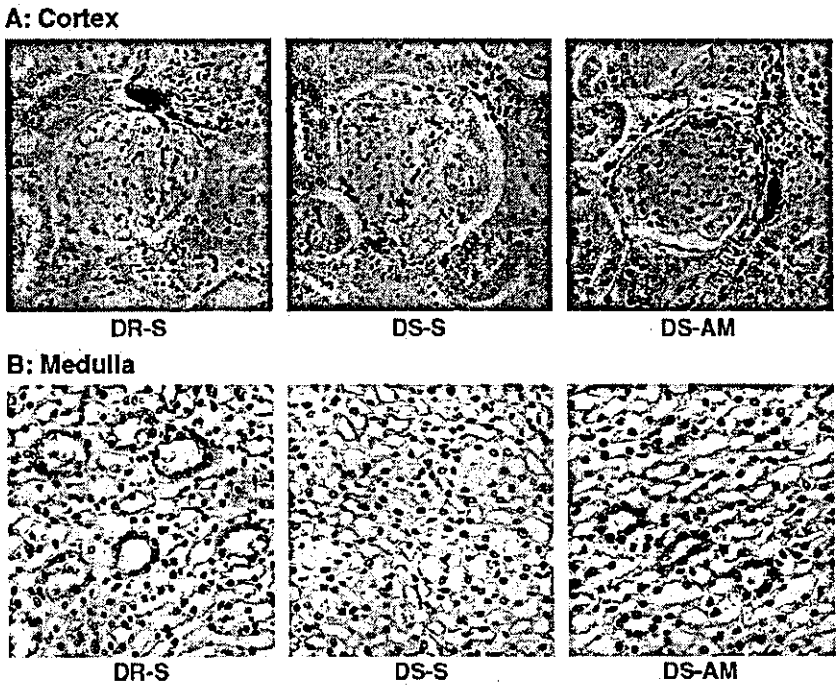


Fig. 3. Neuronal NOS immunoreactivity with a monoclonal antibody in the renal cortex and medulla at the end of the 4th-week in protocol 2.

in a reduction of urinary sodium excretion and an increase of blood pressure in DS rats. The expression of nNOS mRNA and immunoreactivity has been reported to exist in the macula densa and inner medullary collecting duct [19] in rats and renal nNOS specific activity was lower in DS rats than DR rats after a high sodium diet [5]. Interestingly, nNOS specific inhibition made the normally DR rats salt sensitive [20] and high sodium diet induced an increase in nNOS expression in the renal inner medulla of salt-resistant Sprague–Dawley rats [21]. Therefore, we evaluated the expression of nNOS. We observed a reduction in the nNOS level in the macula densa and inner medullary collecting duct in DS rats in the present Western blot and immunohistochemical analyses. Although we did not evaluate nNOS activity in the present study, our results suggested that one possible mechanism of salt-sensitive hypertension might be the reduced renal nNOS expression in the macula densa and inner medullary collecting duct in DS rats.

NO has been reported to be involved partly in vasodilation [22] and urinary sodium excretion [23] induced by adrenomedullin infusion. Recently, NO has been clarified to promote adrenomedullin gene expression in rat aortic vascular smooth muscle cells [24] and the maximal binding of adrenomedullin to its specific receptor in rat mesangial cells [25], suggesting that an accommodative interaction might exist between adrenomedullin and NO. Since we demonstrated that chronic adrenomedullin infusion attenuated salt-sensitive hypertension in association with the increased medullary eNOS expression and nNOS expression in the macula densa and inner medullary collecting duct, the attenuation of increasing of blood pressure by adrenomedullin infusion might be partly due to the increased eNOS and nNOS expression in the kidneys in DS rats.

In conclusion, our results suggest that chronic adrenomedullin infusion attenuates the increasing of blood pressure and decreases the degree of proteinuria probably in part through the increased renal medullary eNOS and nNOS expression in the macula densa and inner medullary collecting duct in DS rats and that renal adrenomedullin may serve as an endogenous protective mechanism against salt-sensitive hypertension. Our findings may open up the possibility of a new therapeutic strategy using adrenomedullin for salt-sensitive hypertension and renal injury.

## Acknowledgements

Support for this study was provided in part by the Promotion of Fundamental Studies in Health Science of the Organization for Pharmaceutical Safety and Research (OPSR) of Japan, and by Grants-in-aid for Scientific Research (14571044) from Japan Society for the Promotion of the Science.

## References

[1] Morimoto A, Uzu T, Fujii T, Nishimura M, Kuroda S, Nakamura S, et al. Sodium sensitivity and cardiovascular events in patients with essential hypertension. Lancet 1997;350:1734–7.
[2] Shultz PJ, Tolins JP. Adaptation to increased dietary salt intake in the rat. Role of endogenous nitric oxide. J Clin Invest 1993; 91:642–50.
[3] Baylis C, Harton P, Engels K. Endothelial derived relaxing factor controls renal hemodynamics in the normal rat kidney. J Am Soc Nephrol 1990;1:875–81.
[4] Tolins JP, Shultz PJ. Endogenous nitric oxide synthesis determines sensitivity to the pressor effect of salt. Kidney Int 1994; 46:230–6.
[5] Ikeda Y, Saito K, Kim JI, Yokohama M. Nitric oxide synthase isoform activities in kidney of Dahl salt-sensitive rats. Hypertension 1995;26:1030–4.
[6] Kitamura K, Kangawa K, Kawamoto M, Ichiki Y, Nakamura S, Matsuo H, et al. Adrenomedullin: a novel hypotensive peptide isolated from human pheochromocytoma. Biochem Biophys Res Commun 1993;192:553–60.
[7] Ichiki Y, Kitamura K, Kangawa K, Kawamoto M, Matsuo H, Eto T. Distribution and characterization of immunoreactive adrenomedullin in human tissue and plasma. FEBS Lett 1994;338:6–10.
[8] Jougasaki M, Wei C-M, Aarhus LL, Heublein DM, Sandberg SM, Burnett Jr JC. Renal localization and actions of adrenomedullin: a natriuretic peptide. Am J Physiol 1995;268:F657–63.
[9] Nishimatsu H, Suzuki E, Nagata D, Moriyama N, Satonaka H, Walsh K, et al. Adrenomedullin induces endothelium-dependent vasorelaxation via the phosphatidylinositol 3-kinase/Akt-dependent pathway in rat aorta. Circ Res 2001;89:63–70.
[10] Sakata J, Shimokubo T, Kitamura K, Nishizono M, Ichiki Y, Kangawa K, et al. Distribution and characterization of immunoreactive rat adrenomedullin in tissue and plasma. FEBS Lett 1994; 352:105–8.
[11] Gonick HC, Ding Y, Bondy SC, Ni Z, Vaziri ND. Lead-induced hypertension: interplay of nitric oxide and reactive oxygen species. Hypertension 1997;30:1487–92.
[12] Suga SI, Phillips MI, Ray PE, Raleigh JA, Vio CP, Kim YG, et al. Hypokalemia induces renal injury and alterations in vasoactive mediators that favor salt sensitivity. Am J Physiol Renal Physiol 2001;281:F620–9.
[13] Khan AI, Kato J, Kitamura K, Kangawa K, Eto T. Hypotensive effect of chronically infused adrenomedullin in conscious Wistar–Kyoto and spontaneously hypertensive rats. Clin Exp Pharmacol Physiol 1997;24:139–42.
[14] Lainchbury JG, Cooper GJ, Coy DH, Jiang NY, Lewis LK, Yandle TG, et al. Adrenomedullin: a hypotensive hormone in man. Clin Sci (Lond) 1997;92:467–72.
[15] Jougasaki M, Aarhus LL, Heublein DM, Sandberg SM, Burnett Jr JC. Role of prostaglandins and renal nerves in the renal actions of adrenomedullin. Am J Physiol 1997;272:F260–6.
[16] Kone BC, Baylis C. Biosynthesis and homeostatic roles of nitric oxide in the normal kidney. Am J Physiol 1997;272:F561–78.
[17] Kurtz A, Gotz KH, Hamann M, Sandner P. Mode of nitric oxide action on the renal vasculature. Acta Physiol Scand 2000;168:41–5.
[18] Ren YL, Garvin JL, Carretero OA. Role of macula densa nitric oxide and cGMP in the regulation of tubuloglomerular feedback. Kidney Int 2000;58:2053–60.
[19] Marsden PA, Hall AV, Brenner BM. Reactive nitrogen and oxygen intermediates and the kidney. In: Brenner BM, editor. The kidney, 5th ed. Philadelphia: WB Saunders; 1996. p. 719–21.
[20] Tan DY, Meng S, Manning Jr RD. Role of neuronal nitric oxide synthase in Dahl salt-sensitive hypertension. Hypertension 1999; 33:456–61.
[21] Mattson DL, Higgins DJ. Influence of dietary sodium intake on renal medullary nitric oxide synthase. Hypertension 1996;27:688–92.

[22] Hirata Y, Hayakawa H, Suzuki Y, Suzuki E, Ikenouchi H, Kohmoto O, et al. Mechanisms of adrenomedullin-induced vasodilation in the rat kidney. Hypertension 1995;25:790–5.
[23] Majid DS, Kadowitz PJ, Coy DH, Navar LG. Renal responses to intra-arterial administration of adrenomedullin in dogs. Am J Physiol 1996;270:F200–5.
[24] Hofbauer KH, Schoof E, Kurtz A, Sandner P. Inflammatory cytokines stimulate adrenomedullin expression through nitric oxide-dependent and-independent pathways. Hypertension 2002;39:161–7.
[25] Dotsch J, Schoof E, Schocklmann HO, Brune B, Knerr I, Repp R, et al. Nitric oxide increases adrenomedullin receptor function in rat mesangial cells. Kidney Int 2002;61:1707–13.

Journal of the American College of Cardiology
© 2005 by the American College of Cardiology Foundation
Published by Elsevier Inc.

Vol. 45, No. 4, 2005
ISSN 0735-1097/05/$30.00
doi:10.1016/j.jacc.2004.10.067

# C-Type Natriuretic Peptide, a Novel Antifibrotic and Antihypertrophic Agent, Prevents Cardiac Remodeling After Myocardial Infarction

Takeshi Soeki, MD,* Ichiro Kishimoto, MD,* Hiroyuki Okumura, MD,* Takeshi Tokudome, MD,* Takeshi Horio, MD,† Kenji Mori, PHD,* Kenji Kangawa, PHD*

*Suita, Osaka, Japan*

**OBJECTIVES** We assessed the hypothesis that in vivo administration of C-type natriuretic peptide (CNP) might attenuate cardiac remodeling after myocardial infarction (MI) through its antifibrotic and antihypertrophic action.

**BACKGROUND** Recently, we have shown that CNP has more potent antifibrotic and antihypertrophic effects than atrial natriuretic peptide (ANP) in cultured cardiac fibroblasts and cardiomyocytes.

**METHODS** Experimental MI was induced by coronary ligation in male Sprague-Dawley rats; CNP at 0.1 μg/kg/min (n = 34) or vehicle (n = 35) was intravenously infused by osmotic mini-pump starting four days after MI. Sham-operated rats (n = 34) served as controls. After two weeks of infusion, the effects of CNP on cardiac remodeling were evaluated by echocardiograpic, hemodynamic, histopathologic, and gene analysis.

**RESULTS** C-type natriuretic peptide markedly attenuated the left ventricular (LV) enlargement caused by MI (LV end-diastolic dimension, sham: 6.7 ± 0.1 mm; MI+vehicle; 8.3 ± 0.1 mm; MI+CNP: 7.7 ± 0.1 mm, $p < 0.01$) without affecting arterial pressure. Moreover, there was a substantial decrease in LV end-diastolic pressure, and increases in $dP/dt_{max}$, $dP/dt_{min}$, and cardiac output in CNP-treated MI rats compared with vehicle-treated MI rats. Importantly, CNP infusion markedly attenuated an increase in morphometrical collagen volume fraction in the noninfarct region (sham: 3.1 ± 0.2%; MI+vehicle: 5.7 ± 0.5%; MI+CNP: 3.9 ± 0.3%, $p < 0.01$). In addition, CNP significantly reduced an increase in cross-sectional area of the cardiomyocytes. These effects of CNP were accompanied by suppression of MI-induced increases in collagen I, collagen III, ANP, and β-myosin heavy chain messenger ribonucleic acid levels in the noninfarct region.

**CONCLUSIONS** These data suggest that CNP may be useful as a novel antiremodeling agent. (J Am Coll Cardiol 2005;45:608–16) © 2005 by the American College of Cardiology Foundation

The mammalian natriuretic peptide system consists of three structurally homologous peptides, atrial natriuretic peptide (ANP), brain natriuretic peptide (BNP), and C-type natriuretic peptide (CNP) (1). The actions of the natriuretic peptides are modulated through membrane-bound receptors, two of which are guanylyl cyclase (GC)-coupled receptors (GC-A and GC-B). These receptors are linked to the cyclic guanosine monophosphate (cGMP)-dependent signaling cascade and mediate the biological actions of the peptides (2). Atrial natriuretic peptide and BNP are mainly released from the heart to act as circulating hormones, which bind to their specific receptor, GC-A, in the vascular tissue, kidney, and adrenal gland and induce vasodilation, natriuresis, and diuresis (3). C-type natriuretic peptide, which was originally isolated from porcine brain extracts (4), not only acts in the central nervous system, but also plays a role in the local regulation such as the suppression of neointimal formation after vascular injury (5) through its specific receptor, GC-B. Recently, we have shown that CNP was synthesized in cultured cardiac fibroblasts and that CNP inhibited both deoxyribonucleic acid (DNA) and collagen synthesis of cardiac fibroblasts more potently than ANP and BNP (6). C-type natriuretic peptide also has more potent antihypertrophic effects than ANP in cultured cardiomyocytes (7). These findings might be due to the relative abundance of GC-B over GC-A in cardiac fibroblasts and in cardiomyocytes (6,7). In addition, in a recent clinical study, CNP was produced by the hearts of patients with chronic heart failure, and its level in the coronary sinus correlated with mean pulmonary wedge pressure (8). These basic and clinical results suggest that CNP might represent an important local mediator in the heart.

Left ventricular (LV) remodeling after myocardial infarction (MI) is a major cause of subsequent heart failure and death (9). Postinfarction remodeling has been divided into an early phase (within 72 h), which involves expansion of the infarct zone, and a late phase (after 72 h), which is associated with time-dependent LV dilation, mural hypertrophy, and cardiac fibrosis (10). Given the inhibitory effects of CNP on cardiac fibrosis and hypertrophy in vitro, CNP might act against the progression of cardiac late remodeling after MI. Furthermore, because intravenously administered CNP has been demonstrated to have much less potent

From the *Department of Biochemistry, National Cardiovascular Center Research Institute, Suita, Osaka, Japan; and the †Department of Medicine, National Cardiovascular Center, Suita, Osaka, Japan. This work was supported, in part, by research grants from the Japanese Ministry of Education, Science, and Culture; the Japanese Ministry of Health, Labor and Welfare; the Program for Promotion of Fundamental Studies in Health Sciences of Pharmaceuticals and Medical Devices Agency; the Japan Cardiovascular Research Foundation; and the Kowa Life Science Foundation.

Manuscript received May 28, 2004; revised manuscript received October 22, 2004, accepted October 25, 2004.

**Abbreviations and Acronyms**

ANP = atrial natriuretic peptide
BNP = brain natriuretic peptide
CNP = C-type natriuretic peptide
cGMP = cyclic guanosine monophosphate
GC = guanylyl cyclase
LV = left ventricle/ventricular
MHC = myosin heavy chain
MI = myocardial infarction
PKG = cyclic guanosine monophosphate-dependent protein kinase
RV = right ventricle/ventricular
TGF = transforming growth factor

vasorelaxant and natriuretic activities than ANP (4,11), CNP is not expected to perturb systemic hemodynamics after massive MI while ANP or BNP is. However, there has been no in vivo evidence to directly prove these beneficial effects of CNP after MI. Therefore, in the present study, we have assessed the hypothesis that in vivo administration of CNP might attenuate cardiac late remodeling after MI. In addition, to elucidate the mechanism involved in the antifibrotic action of CNP, we investigated the action of cGMP/cGMP-dependent protein kinase (PKG) pathway on collagen synthesis by cardiac fibroblasts in vitro, and to clarify whether CNP is an important local mediator in the heart, we investigated the degree and source of endogenous CNP production in the infarcted heart.

## METHODS

**Model of MI.** All experimental procedures were performed according to the guidelines for animal experimentation of National Cardiovascular Center. Male Sprague-Dawley rats (Nihon SLC, Hamamatsu, Japan) weighing 180 to 220 g were anesthetized with sodium pentobarbital (30 mg/kg, intraperitoneally). After left thoracotomy, the left coronary artery was ligated 2 to 3 mm from its origin using a 6-0 Prolene suture. The chest was closed, and the rats were allowed to recover. Sham-operated rats underwent the identical surgical procedure as described above without the actual coronary artery ligation.

**Administration of CNP.** Four days after coronary ligation, the rats with MI were randomly divided into two groups: one to be infused with synthetic CNP (MI+CNP, n = 36) and the other with vehicle (MI+vehicle, n = 42). The CNP group was then fitted with subcutaneous osmotic minipumps (model 2ML2, Alza Corp., Palo Alto, California) filled with synthetic CNP dissolved in a 5% glucose solution and set to release 0.1 μg/kg/min of the peptide for two weeks. The dose of CNP was chosen because our preliminary study revealed that CNP at this dose has no effects on arterial blood pressure and heart rate in rats. Glucose solution was infused in a similar manner in the control group. The pumps were connected to the left jugular vein by a polyethylene catheter. The synthetic CNP was kindly provided by Daiichi Suntory Pharma (Tokyo, Japan).

**Noninvasive blood pressure and pulse rate.** Systolic blood pressure and pulse rate were measured before MI and one day, one week, and two weeks after MI by the tail-cuff method without use of anesthesia (Softron, Tokyo, Japan).

**Echocardiographic and hemodynamic studies.** Echocardiographic studies were performed using an echocardiographic system equipped with a 15-MHz phased-array transducer (SONOS 5500, Hewlett Packard, Andover, Massachusetts) under anesthesia with sodium pentobarbital (30 mg/kg, intraperitoneally) 4 and 18 days after the experimental MI or sham operation as described previously (12). Rats with >20% fractional shortening or an early filling wave (E) velocity to atrial filling wave (A) velocity ratio of <3 in the echocardiographic study performed four days after MI were excluded from the study.

Eighteen days after the coronary ligation or sham operation, hemodynamic studies were performed under anesthesia as previously described (12). After completion of hemodynamic measurements, the hearts were arrested by the injection of 30 mM potassium chloride through the carotid artery, excised, and weighed.

**Histological examination.** After fixation, three cross-sections through the ventricles were obtained and embedded (n = 17 to 19 in each group). Paraffin sections (2 μm) were stained with Masson's trichrome for measurement of infarct size, hematoxylin and eosin for measurement of myocyte size, and Sirius red F3BA for determination of collagen volume fraction. The infarct size was expressed as previously described (13). For the measurement of cardiomyocyte cross-sectional area and diameter in the noninfarcted LV, a total of 30 myocytes sectioned transversely for area and longitudinally for diameter at the level of the nucleus were randomly chosen from each section at ×400 magnification, and traced. To measure collagen volume fraction, 16 fields in the border and remote myocardium of the noninfarcted LV and right ventricle (RV) walls per section were scanned at a magnification of ×200. The interstitial collagen volume fraction was measured while omitting fibrosis of the perivascular, epi-, and endocardial areas from the study. The collagen volume fraction was obtained by calculating the mean ratio of connective tissue to the total tissue area of all the measurements of the section. The collagen-positive areas from all sections were determined by a single investigator who was unaware of the experimental groups.

**Northern blot analysis.** Total ribonucleic acid (10 μg/lane) was extracted from the RV, noninfarcted LV, and infarcted LV (n = 10 in each group). Hybridization was carried out with cDNA probes for rat α-1 (type I) collagen, rat α-1 (type III) collagen, rat fibronectin, rat transforming growth factor (TGF)-β-1, rat ANP, and rat glyceraldehyde-3-phosphate dehydrogenase (GAPDH). We also used synthetic oligonucleotide probes for the α- and β-myosin heavy chain (MHC) messenger ribonucleic

JACC Vol. 45, No. 4, 2005
February 15, 2005:608–16

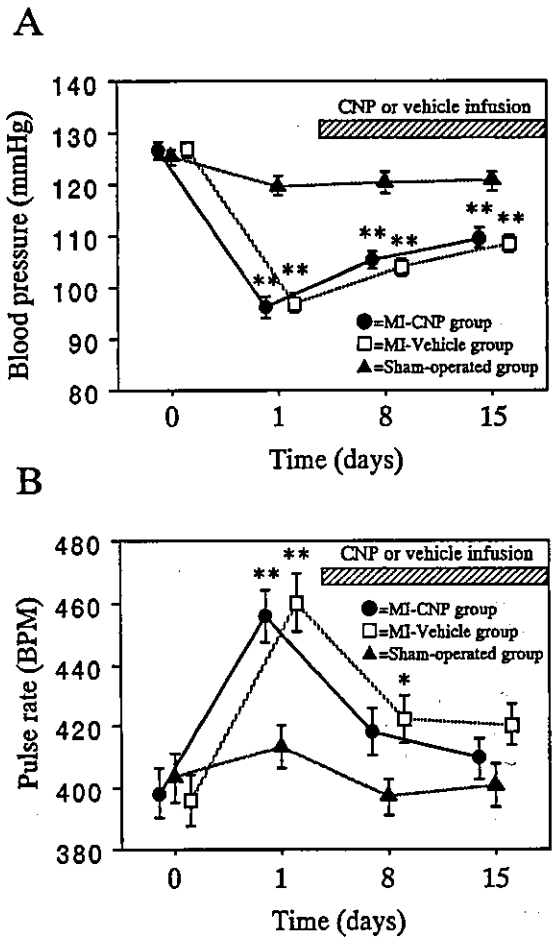


**Figure 1.** Time course of systolic blood pressure (A) and pulse rate (B) in sham-operated rats (**closed triangles**) and in rats with myocardial infarction (MI) before and during infusion of 0.1 μg/kg/min C-type natriuretic peptide (CNP) (**closed circles**) or vehicle (5% glucose solution) (**open squares**). Values are mean ± SEM. A p value for systolic blood pressure by two-way analysis of variance: group <0.001; time course <0.001; group/time course interaction <0.001, and a p value for pulse rate by two-way analysis of variance: group <0.05; time course <0.001; group/time course interaction <0.01. **p < 0.01, *p < 0.05 compared with the sham-operated group at same stage by Bonferroni multiple-comparison *t* test. BPM = beats/min.

acids (mRNA). The band intensity was estimated by a radioimage analyzer (BAS-5000, Fuji Film, Tokyo, Japan).

**Collagen synthesis in vitro.** Neonatal cardiac fibroblasts were prepared as described previously (14). The effects of CNP and a cGMP analog on collagen synthesis in cardiac fibroblasts were evaluated on subconfluent cultures by the incorporation of [$^3$H]proline into cells as previously described (6). In brief, after the preconditioning period, CNP with or without Rp-8-pCPT-cGMP (Calbiochem, San Diego, California), or 8-Bromo cGMP (Sigma, St. Louis, Missouri) was added, and 0.5 μCi of [$^3$H]proline was also added. After the cells were incubated for 24 h, the radioactivity of aliquots of the trichloroacetic acid-insoluble material was determined using a liquid scintillation counter.

**Table 1.** Echocardiographic Parameters

| | Sham | MI+Vehicle | MI+CNP |
|---|---|---|---|
| 4th day (before treatment) | | | |
| AWT diastole, mm | 1.2 ± 0.01 | 1.0 ± 0.01* | 1.0 ± 0.01* |
| PWT diastole, mm | 1.3 ± 0.01 | 1.3 ± 0.01 | 1.3 ± 0.01 |
| LVDd, mm | 6.4 ± 0.1 | 7.0 ± 0.1* | 7.0 ± 0.1* |
| FS, % | 34 ± 1 | 16 ± 0.3* | 15 ± 0.3* |
| E velocity, cm/s | 89 ± 3 | 102 ± 2* | 103 ± 3* |
| A velocity, cm/s | 49 ± 2 | 18 ± 1* | 19 ± 1* |
| E/A | 1.9 ± 0.1 | 5.8 ± 0.2* | 5.6 ± 0.1* |
| 18th day (after treatment) | | | |
| AWT diastole, mm | 1.2 ± 0.01 | 0.9 ± 0.02* | 0.9 ± 0.01* |
| PWT diastole, mm | 1.3 ± 0.01 | 1.5 ± 0.02* | 1.4 ± 0.02*† |
| LVDd, mm | 6.7 ± 0.1 | 8.3 ± 0.1* | 7.7 ± 0.1*† |
| FS, % | 35 ± 1 | 16 ± 0.4* | 18 ± 0.4*† |
| E velocity, cm/s | 88 ± 2 | 112 ± 3* | 102 ± 3*‡ |
| A velocity, cm/s | 51 ± 2 | 19 ± 1* | 26 ± 1*† |
| E/A | 1.8 ± 0.05 | 6.2 ± 0.2* | 4.2 ± 0.2*† |

Values are mean ± SEM. *p < 0.01 compared with sham-operated group; †p < 0.01, ‡p < 0.05 compared with MI+vehicle group by analysis of variance and Bonferroni multiple-comparison t test.

A = atrial filling wave; AWT = anterior wall thickness; CNP = C-type natriuretic peptide; E = early filling wave; FS = fractional shortening; LVDd = left ventricular end-diastolic dimensions; MI = myocardial infarction; PWT = posterior wall thickness.

**Quantitative reverse transcription-polymerase chain reaction.** Endogenous mRNA expressions of ventricular CNP were evaluated in rats killed on day 3, 7, and 18 after MI (without CNP treatment) and on day 3 after sham operation (n = 6 in each group) with quantitative reverse transcription-polymerase chain reaction using a LightCycler system (Roche Applied Science, Penzberg, Germany) according to the manufacturer's instruction.

**Immunohistochemical analysis.** Immunohistochemical studies were performed to localize endogenous CNP in LV myocardium after MI. The section on day 7 after MI (in rats without CNP treatment) was stained with goat anti-CNP antibody (Santa Cruz Biotechnology, Santa Cruz, California) followed by Alexa-Fluor donkey anti-goat IgG antibody (Molecular Probes, Eugene, Oregon) and stained with rabbit fibronectin antibody (Sigma, St. Louis, Missouri) followed by tetrarhodamine isothiocyanate-conjugated goat anti-rabbit IgG antibody (DakoCytomation, Glostrup, Denmark).

**Statistical analysis.** All values are expressed as mean ± SEM. Differences among the groups were evaluated by one-way analysis of variance and two-way analysis of variance for repeated measurements, as appropriate. When a statistical difference was detected by analysis of variance, the Bonferroni method of adjusting for multiple pairwise comparisons was used. A value of $p < 0.05$ was considered statistically significant.

## RESULTS

**The effect of CNP on survival rate and infarct size.** Among the MI rats, two of the CNP-infused rats and seven of the vehicle-infused rats died during the two-week infusion period. The survival rate of the MI+CNP group (94%) was higher than that of the MI+vehicle group (83%), but this

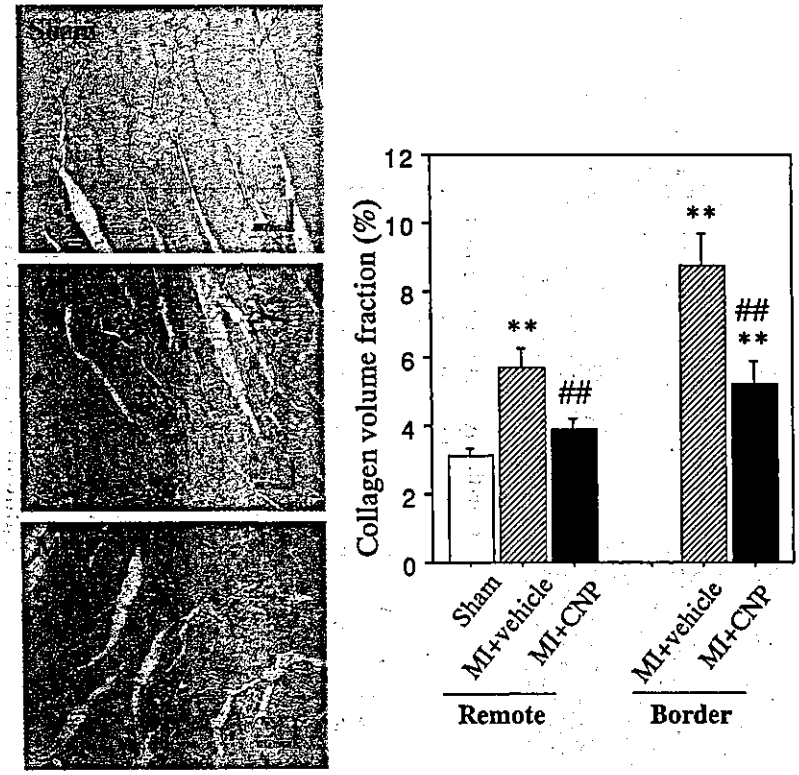


**Figure 2.** The effect of C-type natriuretic peptide (CNP) infusion on collagen volume fraction in the remote and border noninfarcted left ventricular area after myocardial infarction (MI). Representative photomicrographs of collagen volume stained with Sirius red in the remote noninfarcted LV (×200 magnification) **(left)** and quantitative morphometric analysis **(right)**. Values are mean ± SEM. **p < 0.01 compared with the sham-operated group; ##p < 0.01 compared with the MI+vehicle group by analysis of variance and Bonferroni multiple-comparison *t* test.

difference was not statistically significant by Kaplan-Meier survival analysis (p = 0.13). No rats died in the sham group. Therefore, the total numbers for final analysis were 34 rats in the MI+CNP group, 35 in the MI+vehicle group, and 34 in the sham group. There was no difference in infarct size between the MI+CNP and MI+vehicle groups (45 ± 1% and 46 ± 1%, respectively).

**Serial change of noninvasive blood pressure and pulse rate.** A significant reduction in the systolic blood pressure was observed in MI+CNP or MI+vehicle rats compared with the sham-operation rats during two weeks after the operation. As shown in Figure 1A, the systolic blood pressure was not perturbed by CNP infusion at any time points. The pulse rate in MI groups significantly increased at day 1 compared with sham animals and decreased gradually. The pulse rate was not significantly affected by CNP treatment at any time points (Fig. 1B).

**The effect of CNP on echocardiographic and hemodynamic parameters.** Table 1 shows echocardiographic assessments of cardiac geometry and function for the three groups of rats at the 4th and 18th days after MI. At the 4th day (before CNP infusion), when compared with sham, LV enlargement, decreased fractional shortening, and increased ratio of E to A velocities were seen in similar degree in both MI groups. At the 18th day (after two weeks of CNP infusion), hypertrophy of the posterior wall and the LV cavity enlargement caused by MI were significantly attenuated by CNP infusion, although thinning of the anterior wall was not changed; CNP also ameliorated the decrease of fractional shortening. Furthermore, CNP significantly improved LV diastolic filling pattern, resulting in a marked reduction in the ratio of E to A velocities (Table 1).

Table 2 also shows hemodynamic assessments for the three groups of rats at the 18th day after MI. No significant difference was noted in heart rate among the three groups. Mean arterial pressure and LV systolic pressure were lower

**Table 2.** Hemodynamic Parameters

| | Sham | MI+Vehicle | MI+CNP |
|---|---|---|---|
| HR, beats/min | 412 ± 5 | 421 ± 6 | 410 ± 5 |
| MAP, mm Hg | 120 ± 2 | 99 ± 2* | 103 ± 2* |
| LVSP, mm Hg | 139 ± 2 | 116 ± 2* | 118 ± 2* |
| LVEDP, mm Hg | 7 ± 0.4 | 18 ± 1* | 13 ± 1*† |
| LV $dP/dt_{max}$, mm Hg/s | 7,970 ± 156 | 5,019 ± 155* | 5,743 ± 155*† |
| LV $dP/dt_{min}$, mm Hg/s | −6,216 ± 158 | −3,791 ± 151* | −4,644 ± 147*† |
| CO, ml/min | 98 ± 2 | 73 ± 2* | 81 ± 2*† |

Values are mean ± SEM. *p < 0.01 compared with sham-operated group; †p < 0.01 compared with MI+vehicle group by analysis of variance and Bonferroni multiple-comparison *t* test.

CNP = C-type natriuretic peptide; CO = cardiac output; HR = heart rate; LV dP/dt max or min = peak rate of left ventricular rise or fall; LVEDP = left ventricular end-diastolic pressure; LVSP = left ventricular systolic pressure; MAP = mean arterial pressure; MI = myocardial infarction.

JACC Vol. 45, No. 4, 2005
February 15, 2005:608–16

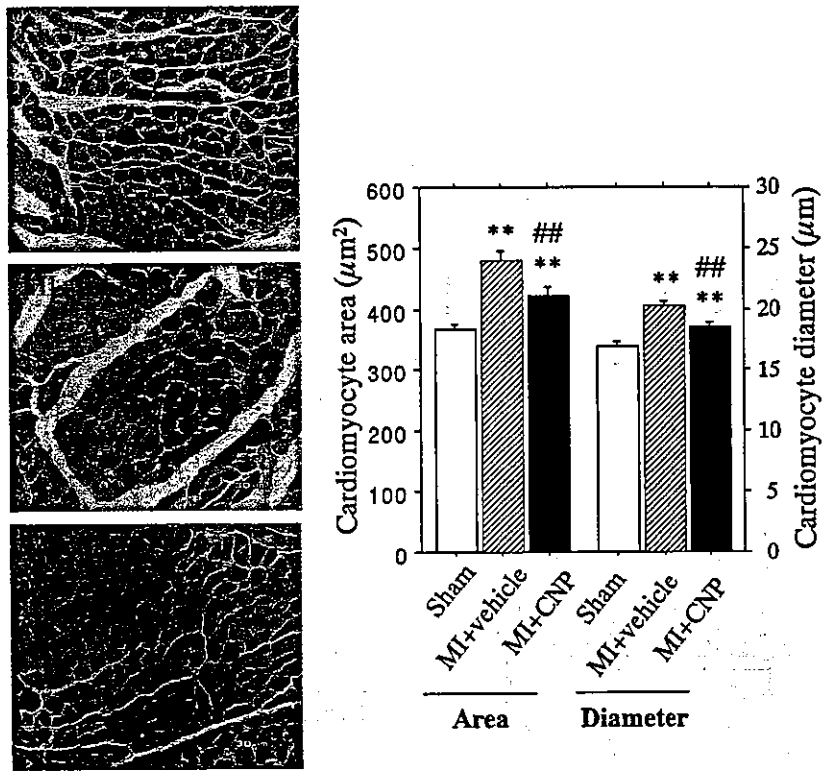


**Figure 3.** The effect of C-type natriuretic peptide (CNP) infusion on cardiac hypertrophy in the noninfarcted left ventricle. Representative photomicrographs of cardiomyocyte size stained with hematoxylin and eosin (×400 magnification) (**left**) and quantitative morphometric analysis of cardiomyocyte area and diameter (**right**). Values are mean ± SEM. **$p < 0.01$ compared with the sham-operated group; ##$p < 0.01$ compared with the myocardial infarction (MI) + vehicle group by analysis of variance and Bonferroni multiple-comparison *t* test.

in the MI+vehicle and MI+CNP groups than in sham, but there were no differences in these parameters between the two MI groups. Left ventricular end-diastolic pressure was higher, and the peak rate of contraction ($dP/dt_{max}$), the peak rate of relaxation ($dP/dt_{min}$), and the cardiac output were lower in MI+vehicle than in sham. As shown in Table 2, the MI-induced systolic and diastolic LV dysfunction was markedly improved by CNP.

**The effect of CNP on cardiac collagen volume and hypertrophy.** To clarify the mechanism of improved cardiac performance caused by CNP, we examined the effects of CNP treatment on collagen volume and mural hypertrophy in the noninfarcted region; CNP significantly ($p < 0.01$) attenuated an increase in morphometrical collagen volume fraction in the remote LV (Fig. 2) and RV (sham: 3.3 ± 0.3%; MI+vehicle: 5.5 ± 0.5%; MI+CNP: 4.2 ± 0.3%). Furthermore, CNP reduced an increase in collagen volume fraction more effectively in the border region of MI, in which fibrosis was more prominent compared with the remote zone (Fig. 2).

The cross-sectional area and diameter of myocytes in the noninfarcted LV significantly increased in MI+vehicle compared with sham, and hypertrophy of the myocytes was significantly ($p < 0.01$) inhibited by CNP infusion (Fig. 3). In agreement with the above results, the heart-weight-to-body-weight ratio, which was increased in the two MI groups compared with sham, was significantly ($p < 0.01$) lowered by CNP treatment (sham: 3.29 ± 0.03 g/kg; MI+vehicle: 3.96 ± 0.09 g/kg; MI+CNP: 3.69 ± 0.06 g/kg).

**The effect of CNP on gene expression.** To confirm the effects of CNP on cardiac remodeling, we examined the expression of several mRNAs associated with fibrosis and hypertrophy in the noninfarcted LV and RV after MI (Figs. 4A, representative autoradiograms, and 4B, quantitative analysis, n = 10 in each group). As shown in Figure 4, the increased mRNA expression of collagen type I and collagen type III after MI was significantly suppressed by treatment with CNP. The increased fibronectin mRNA expression tended to be decreased by CNP, but it was not significant. At the 18th day, mRNA expression of TGF-β-1, which is well known to be a fibrotic cytokine and to be upregulated in the acute phase of MI (15), was not different between MI rats with or without CNP infusion; CNP treatment resulted in suppression of the ANP mRNA level, which is a useful marker of cardiac fetal phenotype modulation after MI, and the β-/α-MHC ratio, which is a qualitative marker of cardiac hypertrophy, in the noninfarcted LV (Fig. 4). In the infarcted LV, mRNA levels of collagen type I, collagen type III, fibronectin, TGF-β-1, ANP, and β-/α-MHC were all increased in the MI+vehicle and MI+CNP groups compared with sham, but there was no difference in these

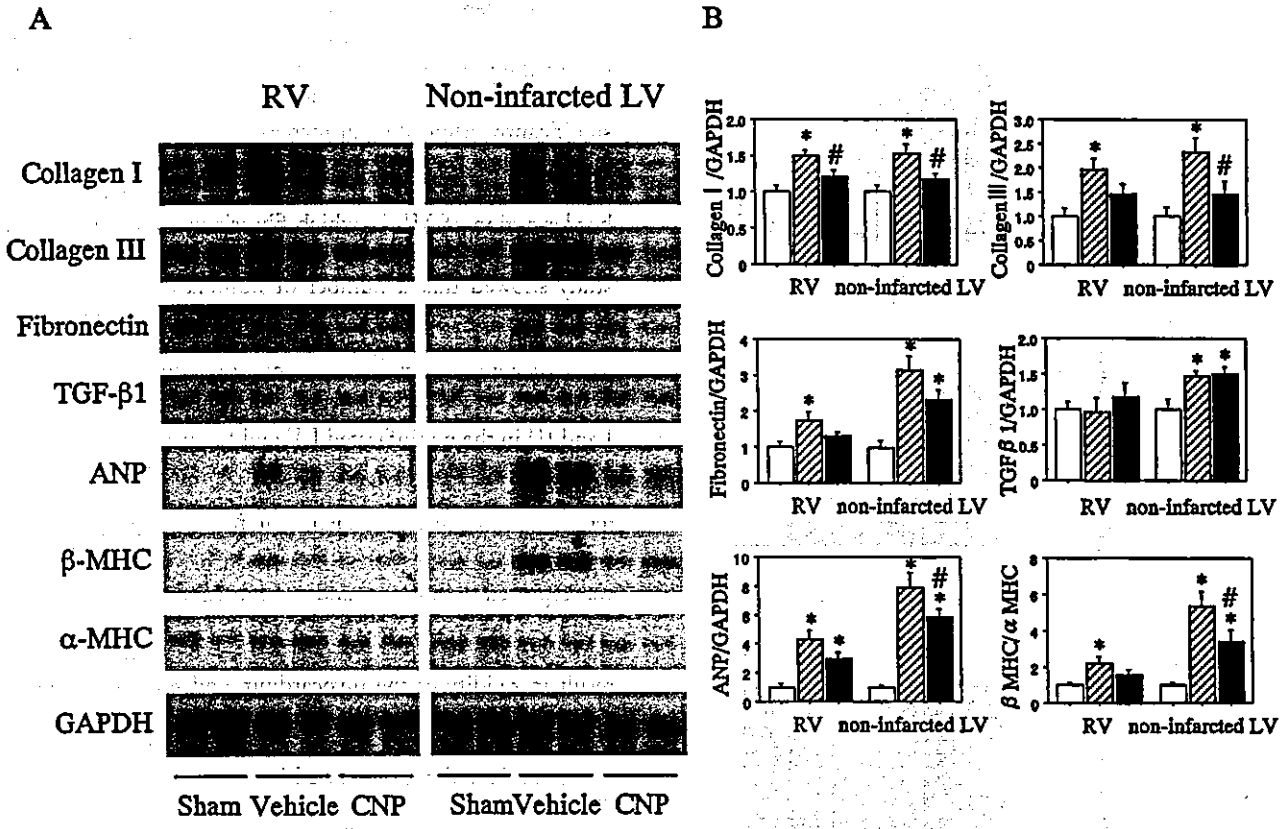


**Figure 4.** The effect of C-type natriuretic peptide (CNP) on messenger ribonucleic acid (mRNA) expression associated with cardiac remodeling after myocardial infarction (MI). **(A)** Typical autoradiograms of Northern blot analysis of mRNA levels in right ventricle (RV) and noninfarcted left ventricle (LV) for collagen type I, collagen type III, fibronectin, transforming growth factor-(TGF)-$\beta$-1, atrial natriuretic peptide (ANP), $\beta$- and $\alpha$-myosin heavy chain (MHC), and glyceraldehyde-3-phosphate dehydrogenase (GAPDH) at the 18th day after MI. **(B)** Quantitative analyses of the abundance of each gene in the RV and noninfarcted LV at the 18th day after MI (n = 10 in each group). In individual samples, each mRNA value was corrected for the GAPDH mRNA value. Levels in sham-operated rats were arbitrarily assigned a value of 1.0. Values are mean ± SEM. $^{**}p < 0.01$, $^{*}p < 0.05$ compared with the sham-operated group; $\#p < 0.05$ compared with the MI+vehicle group by analysis of variance and Bonferroni multiple-comparison *t* test. **Open bars** = sham; **striped bars** = MI+vehicle; **solid bars** = MI+CNP.

parameters in the infarcted LV between the two MI groups (data not shown).

**Cellular mechanism of the antifibrotic action of CNP.** C-type natriuretic peptide and 8-Bromo cGMP, an analog of cGMP, decreased the incorporation of [$^3$H]proline into cardiac fibroblasts in a dose-dependent manner (Figs. 5A and 5B). The decrease of [$^3$H]proline incorporation by CNP was completely blocked by Rp-8-pCPT-cGMP, a cell-permeable inhibitor of PKG type I and type II, at a concentration of $10^{-5}$ mol/l (Fig. 5C).

**Endogenous CNP expression after MI.** C-type natriuretic peptide mRNA expression increased on day 3 by about four-fold in the infarcted LV and two-fold in the noninfarcted LV compared with sham rats, and gradually decreased from day 7 to day 18 (Fig. 6A). C-type natriuretic peptide mRNA expression in RV slightly increased on day 7 only (1.5-fold) (Fig. 6A). In addition, immunohistochemical study revealed that CNP was stained mainly in fibrotic area of the infarct and border region on day 7 after MI (Fig. 6B). These results suggest that endogenous local CNP might play an important role in the infarcted heart.

## DISCUSSION

In this study, we have demonstrated that in vivo administration of CNP improved cardiac function and protected against cardiac remodeling after MI in rats. The beneficial effects of CNP treatment in the heart after MI included attenuation of cardiac fibrosis, hypertrophy, and LV enlargement.

In addition, continuous treatment with CNP had no effects on mean arterial pressure and LV systolic pressure at the time of sacrifice 18 days after MI. The serial change in noninvasive blood pressure during the recovery period after MI was also similar in rats with and without CNP treatment. These findings are consistent with previous studies, which showed that CNP infusion had little vasodepressor or natriuretic activities in rats and healthy humans (4,11).

JACC Vol. 45, No. 4, 2005
February 15, 2005:608–16

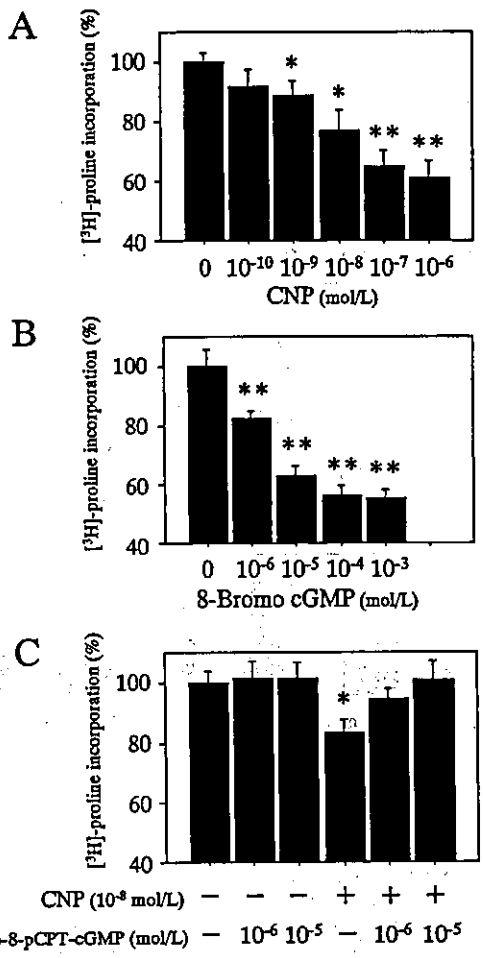


**Figure 5.** The effect of C-type natriuretic peptide (CNP) on collagen synthesis via the cyclic guanosine monophosphate (cGMP)/cyclic guanosine monophosphate-dependent protein kinase (PKG) pathway in cultured neonatal rat cardiac fibroblasts. **(A and B)** The effect of CNP and 8-Bromo cGMP on [$^3$H]proline incorporation in cardiac fibroblasts. **(C)** [$^3$H]proline incorporation in the presence or absence of $10^{-8}$ mol/l CNP with or without Rp-8-pCPT-cGMP, PKG inhibitor. Values are mean ± SEM. $^{**}p < 0.01$, $^{*}p < 0.05$ compared with control by analysis of variance and Bonferroni multiple-comparison *t* test.

Similarly, the heart rate was not significantly affected by CNP infusion throughout the study period.

**The effect of CNP on cardiac performance.** Chronic administration of CNP improved cardiac performance in MI rats, as indicated by increases in LV fractional shortening, cardiac output, and LV $dP/dt_{max/min}$, and by decreases in E/A ratio and LV end-diastolic pressure, which were accompanied by improvement of LV enlargement. Because the effect of CNP on pre- or after-load, heart rate, and infarct size was very little, a mechanism other than hemodynamic improvement or reduction in infarct size is probably the cause of the beneficial effects of CNP on cardiac performance.

**The beneficial effect of CNP on cardiac remodeling through its antifibrotic action.** One possibility is that CNP directly inhibits myocardial fibrosis because we have previously demonstrated that CNP directly inhibited both DNA and collagen synthesis by cardiac fibroblasts in vitro (6). In the present study, we have, therefore, examined the in vivo effect of CNP on fibrosis and found that CNP significantly attenuated an increase in morphometrical collagen volume fraction in the noninfarcted LV and RV. In addition, the effect of CNP was more prominent in the border region of MI, in which fibrosis was more increased, than that in the remote region. Because our preliminary study showed that a number of fibroblasts shift toward a myofibroblastic phenotype indicated by α-smooth muscle actin in the border region of MI, CNP might have more potent inhibitory effect on myofibroblast-like cells than on fibroblasts. Furthermore, the mRNA levels of collagen type I and III in the noninfarcted LV and RV were suppressed by treatment with CNP. These results provide in vivo evidence that CNP is a potent "fibrosis-inhibitory agent" after MI. The amount of myocardial collagen deposition in the infarcted and noninfarcted regions during healing after MI was reported to influence and to be integral to the process of ventricular remodeling (16). In addition, it has been shown that excessive accumulation of myocardial collagen might result in rigidity of the myocardium and severely impaired relaxation (17). Therefore, improved LV $dP/dt_{max/min}$ by CNP after MI might reflect improved myocardial rigidity in the noninfarcted region caused by the reduction in cardiac fibrosis.

Given the in vivo antifibrotic action of CNP, we further explored the cellular mechanisms of this action in vitro. Consistent with our previous study (6), CNP or 8-Bromo cGMP, an analog of cGMP, potently inhibited collagen synthesis of cultured cardiac fibroblasts. In the present study, the inhibitory effect of CNP was completely blocked by Rp-8-pCPT-cGMP, an inhibitor of PKG (Fig. 5), indicating that CNP inhibited collagen synthesis by activating cGMP/PKG pathway.

Some experimental data suggest that antifibrotic agents could potentially enhance the remodeling of the extracellular collagen matrix in the infarct zone during very early stage of healing after MI (18). However, in the present study, the death rate of the MI+CNP group (6%) was lower than that of the MI+vehicle group (17%) during the two-week infusion period, and two dead rats with CNP treatment showed no findings of LV rupture. The late start of CNP infusion at the fourth day of MI might reduce the potential adverse effects of antifibrosis such as wall thinning of infarct zone. Further studies are needed to determine the best timing of CNP treatment after MI.

**The beneficial effect of CNP on cardiac remodeling through its antihypertrophic action.** Another possible mechanism of cardioprotection by CNP might be attenuated myocardial hypertrophy after MI. As shown in the Results section, CNP effectively reduced the MI-induced myocardial hypertrophy in vivo. The findings are in agreement with previous in vitro studies, which showed that natriuretic peptides including CNP prevented hypertrophy

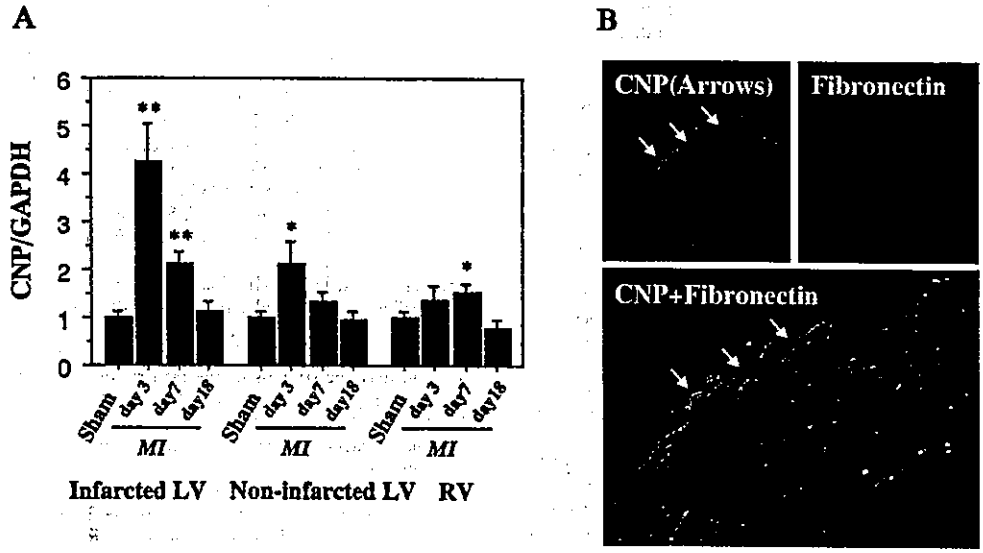


**Figure 6.** Endogenous C-type natriuretic peptide (CNP) expressions after myocardial infarction (MI). **(A)** Endogenous CNP mRNA abundance in the infarcted left ventricle (LV), noninfarcted LV, and right ventricle (RV) at different times after MI and on day 3 after sham operation. Values are mean ± SEM. $^{**}p < 0.01$, $^{*}p < 0.05$ compared with sham by analysis of variance and Bonferroni's multiple-comparison *t* test. **(B)** Immunofluorescent microscopic CNP expression. Upper photomicrographs show the section on day 7 after MI stained by the specific antibody against CNP-53 **(left, green)** and stained by antifibronectin antibody **(right, red)**. Lower photomicrograph shows the merged image (×600 magnification). GAPDH = glyceraldehydes-3-phosphate dehydrogenase.

of cultured cardiomyocytes (7,19). Although the precise mechanism by which CNP inhibits cardiac hypertrophy remains unknown, our previous study (7) suggested that CNP inhibits hypertrophy of cardiac myocytes directly by activating cGMP-dependent mechanism and indirectly by reducing endothelin-1 secretion from nonmyocytes.

On the other hand, because hypertrophy after MI is an adaptive response that offsets increased load, attenuates progressive dilation, and stabilizes contractile function (20), decreased cardiac hypertrophy shown in the present study might be caused by the indirect effect of CNP via decreased LV systolic wall stress. Further studies are needed to determine the contribution ratio of direct and indirect effects of CNP on cardiac hypertrophy.

**Comparison with other antiremodeling therapies after MI.** A number of therapeutic approaches to limiting ventricular remodeling in MI have been reported. These agents include angiotensin-converting enzyme inhibitors, angiotensin II type 1 receptor blockers, β-adrenergic blockers, aldosterone antagonists, and matrix metalloproteinase inhibitors. Although a number of these other agents have been given orally and, in this regard, they have an advantage over CNP, CNP treatment has some advantages concerning short treatment period and fewer side effects. Actually, in previous studies, it took more than four weeks for other agents to attain similar reduction of collagen volume fraction as two weeks treatment of CNP. Furthermore, these synthetic agents might cause harmful effects such as severe hypotension by vasodilators (21) or musculoskeletal toxicity by matrix metalloproteinase inhibitors (22). Because CNP does not affect blood pressure, it can be used in hemodynamically unstable patients as often seen in acute MI.

**Study limitations.** Because the effects of CNP were evaluated after two weeks of therapy in the present study, its long-term effects on the cardiac remodeling after MI remain unclear. For future clinical application, further study is necessary to examine if the antiremodeling effects of CNP persist for the long-term follow-up period.

**Summary.** Our study has demonstrated that continuous administration of CNP improved LV dysfunction and attenuated the development of cardiac remodeling after MI. Because CNP has much weaker vasorelaxant and natriuretic activities, but has much more potent antifibrotic and antihypertrophic actions than ANP or BNP, these beneficial effects of CNP might be associated with direct effects on the failing heart. In conclusion, CNP is potentially useful as a new antiremodeling agent through its novel mechanism of action.

### Acknowledgments

The authors are grateful to Dr. Yujiro Hayashi, Daiichi Suntory Pharma, for the kind gift of CNP. We also thank Ms. Chika Fukuhara for her excellent technical assistance.

**Reprint requests and correspondence:** Dr. Ichiro Kishimoto, Department of Biochemistry, National Cardiovascular Center Research Institute, 5-7-1 Fujishiro-dai, Suita, Osaka 565-8565, Japan. E-mail: kishimot@ri.ncvc.go.jp.

## REFERENCES

1. Rosenzweig A, Seidman CE. Atrial natriuretic factor and related peptide hormones. Annu Rev Biochem 1991;60:229–55.
2. Levin ER, Gardner DG, Samson WK. Natriuretic peptides. N Engl J Med 1998;339:321–8.

3. Nakao K, Ogawa Y, Suga S, et al. Molecular biology and biochemistry of the natriuretic peptide system. I: Natriuretic peptides. J Hypertens 1992;10:907–12.
4. Sudoh T, Minamino N, Kangawa K, Matsuo H. C-type natriuretic peptide (CNP): a new member of natriuretic peptide family identified in porcine brain. Biochem Biophys Res Commun 1990;168:863–70.
5. Furuya M, Miyazaki T, Honbou N, et al. C-type natriuretic peptide inhibits intimal thickening after vascular injury. Ann NY Acad Sci 1995;748:517–23.
6. Horio T, Tokudome T, Maki T, et al. Gene expression, secretion, and autocrine action of C-type natriuretic peptide in cultured adult rat cardiac fibroblasts. Endocrinology 2003;144:2279–84.
7. Tokudome T, Horio T, Soeki T, et al. Inhibitory effect of C-type natriuretic peptide (CNP) on cultured cardiac myocyte hypertrophy: interference between CNP and endothelin-1 signaling pathways. Endocrinology 2004;145:2131–40.
8. Kalra PR, Clague JR, Bolger AP, et al. Myocardial production of C-type natriuretic peptide in chronic heart failure. Circulation 2003; 107:571–3.
9. Hammermeister KE, DeRouen TA, Dodge HT. Variables predictive of survival in patients with coronary artery disease: selection by univariate and multivariate analysis from the clinical, electrocardiographic, exercise, arteriographic, and quantitative angiographic evaluations. Circulation 1979;59:421–30.
10. Sutton MG, Sharpe N. Left ventricular remodeling after myocardial infarction: pathophysiology and therapy. Circulation 2000;101: 2981–8.
11. Igaki T, Itoh H, Suga SI, et al. Effects of intravenously administered C-type natriuretic peptide in humans: comparison with atrial natriuretic peptide. Hypertens Res 1998;21:7–13.
12. Nagaya N, Uematsu M, Kojima M, et al. Chronic administration of ghrelin improves left ventricular dysfunction and attenuates development of cardiac cachexia in rats with heart failure. Circulation 2001;104:1430–5.
13. Fishbein MC, Maclean D, Maroko PR. Experimental myocardial infarction in the rat: qualitative and quantitative changes during pathologic evolution. Am J Pathol 1978;90:57–70.
14. Horio T, Nishikimi T, Yoshihara F, et al. Production and secretion of adrenomedullin in cultured rat cardiac myocytes and nonmyocytes: stimulation by interleukin-1 beta and tumor necrosis factor-alpha. Endocrinology 1998;139:4576–80.
15. Thompson NL, Bazoberry F, Speir EH, et al. Transforming growth factor beta-1 in acute myocardial infarction in rats. Growth Factors 1988;1:91–9.
16. Jugdutt BI, Joljart MJ, Khan MI. Rate of collagen deposition during healing and ventricular remodeling after myocardial infarction in rat and dog models. Circulation 1996;94:94–101.
17. Doering CW, Jalil JE, Janicki JS, et al. Collagen network remodelling and diastolic stiffness of the rat left ventricle with pressure overload hypertrophy. Cardiovasc Res 1988;22:686–95.
18. Jugdutt BI. Ventricular remodeling after infarction and the extracellular collagen matrix: when is enough enough? Circulation 2003;108: 1395–403.
19. Rosenkranz AC, Woods RL, Dusting GJ, Ritchie RH. Antihypertrophic actions of the natriuretic peptides in adult rat cardiomyocytes: importance of cyclic GMP. Cardiovasc Res 2003;57:515–22.
20. Pfeffer MA, Braunwald E. Ventricular remodeling after myocardial infarction. Experimental observations and clinical implications. Circulation 1990;81:1161–72.
21. Jugdutt BI. Myocardial salvage by intravenous nitroglycerin in conscious dogs: loss of beneficial effect with marked nitroglycerin-induced hypotension. Circulation 1983;68:673–84.
22. Drummond AH, Beckett P, Brown PD, et al. Preclinical and clinical studies of MMP inhibitors in cancer. Ann NY Acad Sci 1999;878: 228–35.

*Endocrine Journal* 2004, **51** (6), 569–577

# Identification of 2,3,7,8-Tetrachlorodibenzo-p-dioxin (TCDD)-inducible and -suppressive Genes in the Rat Placenta: Induction of Interferon-regulated Genes with Possible Inhibitory Roles for Angiogenesis in the Placenta

TETSUYA MIZUTANI, MIKI YOSHINO, TOMOKO SATAKE, MIYUKI NAKAGAWA, RYUTA ISHIMURA*, CHIHARU TOHYAMA*, KOICHI KOKAME**, KENJI KANGAWA** AND KAORU MIYAMOTO

*Department of Biochemistry, Faculty of Medical Sciences, University of Fukui, Matsuoka, Fukui 910-1193, Japan; CREST, JST, Kawaguchi 332-0012, Japan*

**Environmental Health Sciences Division, and Endocrine Disruptors and Dioxin Research Project, National Institute for Environmental Studies, 16-2 Onogawa, Tsukuba 305-8506, Japan; CREST, JST, Kawaguchi 332-0012, Japan*

***National Cardiovascular Center Research Institute, 5-7-1 Fujishirodai, Suita, Osaka 565-8565, Japan*

**Abstract.** Exposure to a low dose of 2,3,7,8-tetrachlorodibenzo-p-dioxin (TCDD) results in a variety of toxic manifestations, including fetal death. In order to evaluate the effects of low dose TCDD on placental function, pregnant Holtzman rats were given a single oral dose of 1600 ng TCDD/kg body wt or an equivalent volume of vehicle (control) on gestation day 15 (GD15), and changes in the gene expression in the placenta on GD20 were analyzed by two comprehensive methods, representational difference analysis (RDA) and DNA microarray technology. Candidates of TCDD-inducible and -suppressive genes were selected. Quantitative real-time PCR analysis was then performed to verify the induction or suppression levels of the candidate genes. Finally, we identified 81 TCDD-inducible and 21 TCDD-suppressive genes from the placenta of TCDD-treated Holtzman rats on GD20. One of the remarkable profiles of the gene expression was that glucose transporters were strongly up-regulated by the TCDD treatment. Furthermore, many interferon-inducible genes were also up-regulated by the treatment. They included several cytokines such as IP-10 known as a potent angiogenesis inhibitor. In addition, interferon molecules are known to suppress angiogenesis. The above observations suggest that activation of the interferon signaling pathway and the induction of anti-angiogenic factors by TCDD might have a role in causing the inhibition of neovascularization, resulting in the hypoxic state of placenta and increased incidence of fetal death.

*Key words*: TCDD, Placenta, Gene expression, Real-time PCR, DNA microarray

(*Endocrine Journal* **51**: 569–577, 2004)

**2,3,7,8-Tetrachlorodibenzo-p-dioxin** (TCDD) is known to be the most toxic congener among the dioxin and related compounds found in the environment. Exposure to TCDD causes a diverse spectrum of toxicities in humans and laboratory animals [1–4]. The fetus is one of the most sensitive targets of TCDD and exhibits a wide range of biological responses at low TCDD levels that have no detectable effects on maternal side (usually the levels were ten to hundred times lower than those of LD50). One of the most severe adverse effects of TCDD is intrauterine fetal death [1, 5–7]. The incidence has been shown in all species studied to date, including the monkey, hamster, rat, and mouse. Although fetal death is an important aspect of TCDD toxicity, its precise mechanism is not well understood. Placenta plays a crucial role in maintaining normal fetal growth such as exchange of oxygen and carbohydrate nutrients. In previous studies Ishimura *et al.*

Received: May 28, 2004
Accepted: October 5, 2004
Correspondence to: Dr. Kaoru MIYAMOTO, Department of Biochemistry, Faculty of Medical Sciences, University of Fukui, Matsuoka, Fukui 910-1193, Japan

demonstrated that exposure of pregnant rats to 800 or 1600 ng TCDD/kg on gestational day 15 (GD15) resulted in an increased incidence of fetal death on GD20 [8, 9]. In their experimental protocol, the placenta showed several abnormalities that led to increased risk for fetal death. Exposure to TCDD altered the glucose kinetics in placenta [8] and caused reduced blood flow and placental hypoxia [9], leading them to hypothesize that the increased incidence of the fetal death may be due to reduced blood flow into the placenta [8, 9]. In order to clarify what kind of genes are involved in these placental abnormalities or what other aspects of TCDD toxicities exist in the placenta, we conducted a comprehensive analysis of gene expression in placenta of pregnant Holtzman rats treated with TCDD using representational difference analysis (RDA) and DNA microarray technology. RDA is a subtraction cloning method developed by Pastorian *et al.* [10]. The RDA and the DNA microarray are very powerful and comprehensive methods to identify inducible or suppressive genes by given hormonal or pharmacological treatments. Previously we have reported many gonadotropin-inducible genes in the rat ovary by using those methods [11–13]. In this study, many candidates for placental TCDD-inducible or -suppressive genes were selected by those methods, and the induction or suppression was verified by quantitative real-time PCR.

Profiling analysis of the verified genes revealed that, in addition to the genes involved in the glucose uptake, those involved in the interferon signaling pathway were strongly induced by the TCDD treatment. Based on the results obtained, the molecular mechanisms of placental disorders by low dose TCDD will be discussed.

## Materials and Methods

*Reagents*

2,3,7,8-TCDD was obtained from Cambridge Isotope Laboratory (Andover, MA). Rat cDNA glass array (Gene Chip Rat Expression Array 230A) was from Affymetrix, Inc., Santa Clara, CA.

*Animals*

Holtzman rats were purchased from Harlan Sprague-Dawley (Indianapolis, IN). The animals were maintained in a controlled environment with 12/12 h light/dark cycles, and given free access to laboratory rat chow and water. Female rats were allowed to mate on proestrus overnight, and, if vaginal plugs were observed in the morning, the day was designated GD0. Six pregnant rats were treated with TCDD, and a total of 10 dead fetuses was observed among 83 fetuses. The pregnant rats were housed individually until exercised. All animal experiments were performed according to the guidelines for animal welfare of the National Institute for Environmental Studies [8, 9].

*TCDD treatment*

The pregnant animals were exposed to TCDD as described previously [8, 9]. TCDD was dissolved in nonane at a concentration of 20 μg/ml, and the solution was diluted with corn oil. On GD15 the pregnant rats were given a single oral dose of 1600 ng TCDD/kg body wt or an equivalent volume of mixture of nonane and corn oil solution (control). Placentas were collected from the TCDD treated or control rats on GD20. The placental samples were immediately frozen in liquid nitrogen and maintained at –80°C until used.

*Representational difference analysis*

For isolating TCDD-inducible and -suppressive genes from the placenta, representational difference analysis (RDA) was performed according to the procedure reported by Pastorian *et al.* [10]. Briefly, total RNA was extracted from each placenta. Each five placental RNA samples were mixed and used for further analysis. After Oligo-dT latex beads treatment, mRNA preparations were then converted to respective double-stranded cDNAs. Tester TCDD-treated placental cDNAs and driver control placental cDNAs were digested with a restriction enzyme DpnII. The digested tester cDNA fragments were ligated with first-round adaptor oligonucleotide molecules, and then mixed with the excess amount of the enzyme digested driver cDNAs. The mixture was denatured and then incubated at 67°C for 16 hours for hybridization. After the hybridization, only the tester specific cDNA fragments were amplified by PCR reaction using primers complementary to the adaptor sequence. For the second cycle RDA, the resulting PCR products, in which the tester specific cDNA fragments were enriched, were digested again with DpnII, and then followed by the second adaptor

ligation and hybridization in order to further enrich tester specific cDNA fragments. The PCR products after the second RDA reaction were ligated in to pGEM T-vector, and individual clones were analyzed to identify TCDD-sensitive genes.

*DNA microarray*

The microarray method was carried out according to the manufacturer's instruction.

Briefly, total RNA was extracted from the TCDD-treated and control placentas described above. Double stranded cDNA libraries were constructed from the mRNA of TCDD-treated and the control placentas using an oligo-dT primer with a T7-promoter sequence at the 5'-end. Biotin-labeled complementary RNA was *in vitro* transcribed by T7 polymerase using the cDNA libraries as template. The biotin-labeled RNA was fragmented and hybridized to the Rat cDNA glass array for 16 hr at 45°C and then washed and stained using the GeneChip Fluidics. The array was scanned by a GeneArray scanner, and hybridization patterns were detected as fluorescent light from reporter groups that have been incorporated into the target genes. The average difference measurements computed in the Affymetrix Microarray Analysis Suite 4.0 serve as a relative indicator of the level of expression.

*Quantitative Real-Time PCR*

Messenger RNA was extracted using an RNA extraction solution (Trizol) and oligo-dT latex beads as described previously [11–13]. Five micrograms of mRNA preparations were reverse-transcribed, and then converted to double stranded cDNA molecules. Complementary DNA was quantified by UV absorption measurement, and 1 ng was subjected to the PCR reaction as template. As an internal standard, TATA binding protein (TBP) was used instead of GAPDH, since GAPDH gene expression was affected by the TCDD treatment (data not shown). PCR reaction involved template cDNA samples, Advantage Taq Plus DNA polymerase (Clontech), dNTP, and Syber Green. Serial dilutions of the templates were used to create a concentration curve, and relative expression levels were calculated for each sample [14]. Abundance of each gene was referred to as a Ct (cycle threshold) value in this system.

## Results

Exposure of pregnant Holtzman rats to 1600 ng TCDD/kg on GD15 resulted in an increased incidence of fetal death on GD20 [8, 9]. In these studies, each placenta from the TCDD-treated and control rats was prepared by the same exposure protocol as previous studies [8, 9], and gene expression in the placenta was analyzed by RDA and DNA microarray methods. Generally the RDA method is more sensitive than the DNA microarray, while the latter covers more comprehensive genes than the RDA method. A total of 2536 clones were picked-up and characterized from the RDA-subtracted cDNA libraries as candidate genes. In addition, the same tissues were used for the DNA-microarray, and among 13000 genes spotted on the array, 43 TCDD-inducible and 18 TCDD-suppressive candidate genes (cut-off values of 2.0 as inducible and 0.5 as suppressive genes) were also picked-up. All of these candidate genes picked-up by both methods were verified by using real-time PCR analysis, and genes that showed expression ratios (TCDD-treated/control) of more than 2.0 or less than 0.5 were finally identified as TCDD-sensitive. TCDD-inducible and -suppressive genes in the rat placenta identified by RDA and DNA microarray methods were summarized in Table 1 and Table 2, respectively.

*TCDD-inducible genes in the placenta*

As listed in Table 1, 81 genes were identified as TCDD-inducible genes in the placenta, 22 genes of which were from the results of DNA microarray analysis. Eleven genes were reported only on EST databases, and one gene showed no significant similarity to any gene on DNA databases. Other genes were all annotated as shown in Table 1 including those homologues of human or mouse. They were categorized into several groups. Enzyme genes include CYP1A1 and CYP1B1 that are known as the typical TCDD target genes [15, 16]. Inducible genes in placenta include some of the major blood proteins, such as prealbumin, apolipoproteins, transferrin, retinol-binding protein, prothrombin, and fibrinogens. This suggests that the placental production of the blood proteins was stimulated by the TCDD treatment. In addition, two placental specific genes, alpha-fetoprotein and pregnancy-specific glycoprotein (rnCGM3), were also induced by the TCDD treatment.

**Table 1.** TCDD-inducible genes in the rat placenta

| Molecular function | Description | Array ratio | Real Time PCR ratio | Ct | Accession |
|---|---|---|---|---|---|
| Enzyme | (LMW) K-kininogen | 3.32 | 8.14 | 30.06 | M11884 |
| | (LMW) T-kininogen I | ND | 4.43 | 30.53 | M11883 |
| | Aldolase B | ND | 2.72 | 34.15 | M10149 |
| | Alpha-1-protease inhibitor | ND | 3.37 | 32.17 | D00675 |
| | Alpha-2 antiplasmin | ND | 3.38 | 30.03 | AY216659 |
| | Alpha-fibrinogen | 5.77 | 5.05 | 33.13 | M35601 |
| | Brain 4.1(L) | ND | 2.24 | 29.48 | AB019257 |
| | CYP1A1 | ND | 425.81 | 26.13 | K02246 |
| | CYP1B1 | ND | 3.90 | 34.60 | X83867 |
| | Cathepsin B | ND | 2.11 | 19.33 | X82396 |
| | Creatine kinase-B | ND | 2.62 | 29.12 | M57664 |
| | Cytosolic NADP-dependent isocitrate dehydrogenase | ND | 3.77 | 24.51 | L35317 |
| | Fibrinogen B-beta-chain | 5.87 | 7.95 | 30.89 | M27220 |
| | Glutathione S-transferase Ya subunit | ND | 4.27 | 31.73 | M26874 |
| | NADH dehydrogenase (ubiquinone) Fe-S protein 7 | ND | 2.99 | 26.11 | BC013503 |
| | NC1 protein (nc1 gene) | ND | 2.25 | 28.63 | AJ250730 |
| | Peroxisomal enoyl hydratase-like protein (PXEL) | ND | 2.01 | 22.38 | U08976 |
| | Protein C | 3.91 | 4.10 | 29.36 | X64336 |
| | Prothrombin precursor (F2 gene) | 4.38 | 5.92 | 24.44 | X52835 |
| | RASP1 | ND | 2.52 | 31.93 | U55765 |
| | Stearoyl-CoA desaturase 2 | ND | 2.31 | 29.98 | AB032243 |
| | Tissue factor protein | 1.93 | 2.29 | 25.09 | U07619 |
| Transcription Factor | Zinc finger homeodomain enhancer-binding protein-1 (Zfhep-1) | ND | 2.36 | 32.92 | U51583 |
| Immunity Protein | Da1-24 | 3.17 | 2.64 | — | AY325253 |
| | Interleukin-12 p40 precursor | ND | 1.96 | 35.40 | AF133197 |
| | MHC class I antigen (RT1-E gene) | ND | 2.42 | — | AJ306619 |
| | MHC class I protein | ND | 6.46 | — | L26224 |
| | Pregnancy-specific glycoprotein (mCGM3) | ND | 2.17 | — | U09815 |
| Signal Transducer | Beta ig-h3 | ND | 2.73 | 31.93 | AF305713 |
| | CXC chemokine LIX | ND | 2.60 | 31.90 | U90448 |
| | Inhibin alpha-subunit | ND | 1.98 | 27.41 | M36453 |
| | Interferon beta | ND | 5.07 | 36.92 | D87919 |
| | Interferon inducible protein 10 (IP-10) | 5.03 | 9.48 | 25.38 | U22520 |
| | Macrophage inflammatory protein-2 | ND | 6.29 | 32.48 | AB060092 |
| | Monokine induced by interferon gamma (Mig) | ND | 3.28 | 33.97 | AF537208 |
| | Proliferin-related protein | 1.94 | 1.82 | 24.23 | AF139809 |
| Transporter | Alpha-fetoprotein (AFP) | ND | 5.47 | 27.57 | X02361 |
| | ApolipoproteinA-I | ND | 6.26 | 26.66 | M00001 |
| | Apolipoprotein A-IV | 5.07 | 4.24 | 21.71 | M00002 |
| | Apolipoprotein B | 3.36 | 7.07 | 28.26 | M27440 |
| | Beta-2 glycoprotein I | 5.10 | 6.28 | 30.95 | X15551 |
| | Beta-globin | ND | 3.71 | 13.83 | X16417 |
| | GLUT2 | ND | 7.39 | 31.47 | J03145 |
| | GLUT4 | ND | 2.84 | 31.49 | D28561 |
| | Retinol-binding protein (RBP) | 2.75 | 5.39 | 32.55 | M10934 |
| | Transferrin | 5.89 | 4.12 | 22.82 | X77158 |
| | Transferrin-like | ND | 4.08 | 26.01 | AF476964 |
| Structural Protein and Other Groups | Angiopoietin-related protein 3 | ND | 8.90 | 30.40 | *CB581433 |
| | Claudin 2 | 2.29 | 3.27 | 26.96 | *BM392116 |
| | Collagen alpha 1 type XI | ND | 2.60 | 33.72 | AJ005396 |
| | Collagen type XXVII proalpha 1 chain (col27a1) | ND | 1.98 | 28.20 | AY232999 |

**Table 1.** (continued)

| Molecular function | Description | Array ratio | Real Time PCR ratio | Ct | Accession |
|---|---|---|---|---|---|
| | Decorin | ND | 2.07 | 24.20 | X59859 |
| | Ficolin-B | ND | 2.33 | 29.23 | AB036792 |
| | Glucocorticoid-attenuated response gene 16 | ND | 92.29 | 27.14 | AJ276893 |
| | Glucocorticoid-attenuated response gene 39 | ND | 5.54 | 28.07 | *CB719539 |
| | Hypothetical protein RMT-7 | ND | 2.09 | 23.13 | AF465614 |
| | Interferon-inducible protein homologue | ND | 6.15 | 24.96 | *CB610262 |
| | Interferon, alpha-inducible protein (G1p2) | ND | 2.76 | 23.17 | *CB790136 |
| | Matrix metalloproteinase inhibitor (TIMP-1) | 2.15 | 2.11 | 25.20 | L31883 |
| | Mx1 | 4.51 | 6.41 | 26.00 | X52711 |
| | Mx2 | 3.80 | 7.27 | 25.71 | X52712 |
| | Mx3 | ND | 3.06 | 26.70 | X52713 |
| | Prealbumin | 2.04 | 4.76 | 27.03 | K03252 |
| | Pro alpha 1 collagen type III | ND | 2.56 | 26.78 | X70369 |
| | Proteasome subunit R-RING12 | ND | 2.92 | 27.78 | D10757 |
| | Ribosomal protein L5 | ND | 2.34 | 20.59 | X06148 |
| | Similar to PC-LKC gene product | 1.92 | 2.06 | 27.53 | *BI291884 |
| | Similar to vinculin | ND | 1.99 | 27.73 | *CB757866 |
| | Spp-24 precursor | 3.03 | 6.13 | 25.56 | U19485 |
| | TORID | ND | 2.53 | 25.27 | AF370882 |
| | Thrombospondin | ND | 2.30 | 28.72 | *AB113080 |
| | Type VI collagen alpha3 subunit | 1.92 | 1.94 | 25.49 | *AI176126 |
| Function Unknown | AB113071 | ND | 2.37 | 31.85 | *AB113071 |
| | Clone nrhy5-00111-g2 | ND | 3.17 | 27.96 | *CB546450 |
| | DRNBNB02 | ND | 2.06 | 24.98 | *BG671212 |
| | EST196998 | 1.98 | 2.16 | 30.78 | *AA893195 |
| | LRRGT00077 | ND | 2.29 | 30.17 | *AY387063 |
| | UI-R-BJ0p-afw-e-10-0-UI.r1 | ND | 2.14 | 27.92 | *BF566943 |
| | UI-R-C4-akz-c-07-0-UI.s1 | 3.22 | 2.99 | 24.70 | *AW531805 |
| | UI-R-E0-bq-f-06-0-UI.r1 | ND | 5.64 | 30.34 | *BF550478 |
| | Unknown | ND | 2.05 | 26.30 | ND |

ND: Not determined, Ct: cycle threshold, *: Rat EST database

Two characteristic profiles of the induction were (1) glucose transporters and (2) interferon-related genes, details of which will be described elsewhere.

*TCDD-suppressive genes in the placenta*

As listed in Table 2, 21 genes were identified as TCDD-suppressive genes in the placenta, 10 genes of which were from the results of the DNA microarray analysis. Six genes were reported only on EST databases, and three genes showed no significant similarity to any gene on existing DNA databases. Other genes were all annotated as shown in Table 2 including those homologues of human or mouse.

*Induction of glucose transporter family genes*

As shown in Fig. 1, expressions of four major glucose transporter genes were examined. Quantitative real-time PCR revealed that GLUT2 and GLUT4 were strongly induced by the TCDD treatment in the placenta. Gene expression of GLUT3 was also marginally increased by the treatment (1.58-fold), but that of GLUT1 was less affected (1.24-fold). In the control placenta, GLUT3 was abundantly expressed (Ct26.57), while expression levels of the other three transporter genes were relatively low (Ct32.73 for GLUT1, Ct31.47 for GLUT2, and Ct31.49 for GLUT4). Therefore, in addition to the remarkable induction of GLUT2 and GLUT4 genes, a small but significant increase in GLUT3 gene expression may have a major physiolog-

**Table 2.** TCDD-suppressive genes in the rat placenta

| Molecular function | Description | Array ratio | Real Time PCR ratio | Ct | Accession |
|---|---|---|---|---|---|
| Enzyme | Urokinase-type plasminogen activator | 0.48 | 0.45 | 27.99 | X63434 |
| | LASP-1 | ND | 0.19 | 25.46 | AF242187 |
| Signal Transducer | Hepatic product spot 14 | 0.43 | 0.33 | 31.78 | K01934 |
| | Prepronociceptin | 0.59 | 0.63 | 25.84 | X97375 |
| | Prolactin-like protein H | 0.50 | 0.41 | 27.74 | AB009889 |
| Transcription Factor | Transcription factor GATA-1 | 0.55 | 0.47 | 31.50 | D13518 |
| | Zinc finger protein 52 | ND | 0.16 | 34.17 | *CK470357 |
| Transporter | mBLVR | ND | 0.54 | 25.50 | *CB557112 |
| Structural Protein and Other Groups | Talin | ND | 0.35 | 26.13 | *CK366133 |
| Function Unknown | Ab2-225 | 0.56 | 0.60 | 27.78 | AY325197 |
| | BB857172 | ND | 0.16 | 29.50 | *BB857172 |
| | Clone mrpe4-00034-a12 | ND | 0.16 | 32.27 | *CB760299 |
| | Eker rat-associated intracisternal-A | ND | 0.43 | 32.27 | U23776 |
| | EST224029 | 0.59 | 0.62 | 24.96 | *AI180286 |
| | FAD104 | ND | 0.49 | 25.21 | *CB702955 |
| | Nuclear-localized inactive X-specific transcript (Xist) | 0.27 | 0.33 | 27.18 | *AI228978 |
| | UI-R-BJ1-auz-g-11-0-UI.s1 | ND | 0.31 | 25.56 | *BE111117 |
| | UI-R-CX0s-cct-f-09-0-UI.s1 | 0.43 | 0.54 | 27.16 | *BI284907 |
| | Unknown mRNA | 0.43 | 0.48 | 26.53 | AF152002 |
| | Unknown | ND | 0.45 | 31.31 | ND |
| | Unknown | ND | 0.51 | 24.21 | ND |

ND: Not determined, Ct: Cycle threshold, *: Rat EST database

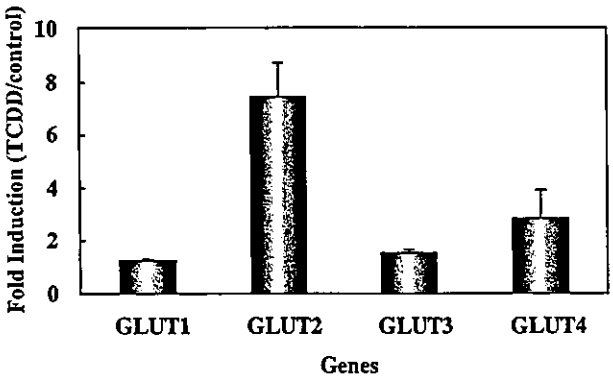


**Fig. 1.** Induction of glucose transporter genes in the rat placenta by TCDD.
Expression levels of major 4 glucose transporter genes were determined by quantitative real-time PCR, and changes in the expression levels were compared. Values were expressed as fold induction (TCDD/control). Serial dilutions of five points for each sample were used to make each dilution curve. TATA binding protein (TBP) was used as an internal standard to ensure equal loading of template cDNA molecules.

ical significance of the glucose-uptake in the TCDD-treated placenta.

*Induction of interferon-related genes*

One of the most remarkable findings of the pesent experiment was that many interferon-regulated genes were induced in the placenta of TCDD-treated animals. As shown in Fig. 2, 15 out of 18 interferon-inducible genes examined were strongly up-regulated by the TCDD treatment. Among them were interferon-inducible cytokines, such as IP-10 [17, 18], macrophage inflammatory protein-2, monokine induced by gamma interferon (Mig) [19] and CXC chemokine LIX [20]. Of these, IP-10 was reported to be involved in the interferon-mediated inhibition of angiogenesis [17, 18]. Since many interferon-inducible genes were up-regulated by the TCDD-treatment, we examined the levels of interferon family genes. At the transcription levels, the interferon beta gene was up-regulated (5.07-fold induction) in the TCDD-treated placenta (Table. 1), but we were not able to detect interferon-alpha and -gamma genes in our system (data not shown).

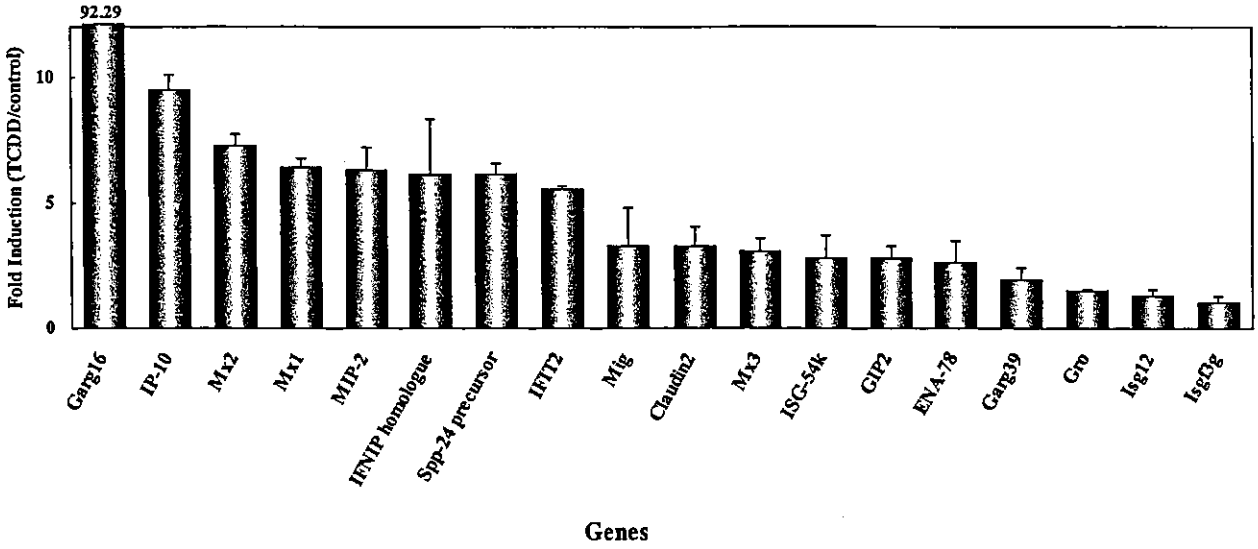


**Fig. 2.** Induction of interferon regulated genes in the rat placenta by TCDD.
Expression levels of 18 interferon regulated genes were determined by quantitative real-time PCR, and changes in the expression levels were compared. Values were expressed as fold induction (TCDD/control). Serial dilutions of five points for each sample were used to make each dilution curve. TATA binding protein (TBP) was used as an internal standard to ensure equal loading of template cDNA molecules.

## Discussion

Previous studies have shown that a very low dose of TCDD results in the increased incidence of fetal death [8, 9]. Histological and protein profiling analysis revealed that the fetal death after the TCDD treatment may be due to the placental hypoxia [9]. In order to evaluate further the mechanisms of the induction of such the adverse effect, comprehensive analysis was done to examine changes in the placental gene expression. As clearly shown in Fig. 1, glucose transporter genes were all induced after the TCDD treatment. Ishimura *et al.* previously reported the histopathological changes in glycogen cells and the elevated levels of glucose content and GLUT3 mRNA expression in the placenta of the TCDD-exposed rats in comparison to those of the control rats [9]. In addition to GLUT3 mRNA, we showed here that GLUT2 and GLUT4 mRNAs were strongly induced by the TCDD-treatment, and that GLUT1 mRNA was less affected by the treatment, indicating that most of major glucose transporter genes were up-regulated by TCDD, which may lead to glycogen accumulation in the placenta. In our quantitative real-time PCR system, values of cycle threshold (Ct) represent expression levels of genes. The Ct value of GLUT3 mRNA was much lower than those of other GLUT family genes, suggesting that the major glucose transporter working in the placenta may be GLUT3, though strong induction of GLUT2 and GLUT4 genes may also play significant roles in the glucose accumulation in the TCDD-treated placenta. As far as we know, this is the first report describing that GLUT2 and GLUT4 genes were actually expressed in the placenta under specific conditions such as the TCDD treatment. It is likely that a tissue-specific responsive mechanism of TCDD exists for the induction of glucose transporters in the placenta, since those transporter genes were not up-regulated in other tissues such as the ovary from the same TCDD-treated animals (data not shown). Histological studies by Ishimura *et al.* showed that blood vessel formation in the placenta was severely impaired by the TCDD treatment (unpublished data), indicating that the angiogenesis was inhibited in the placentas of TCDD-treated animals on GD20. Therefore, the TCDD treatment may cause hypoxic conditions in placenta. It was reported that the expression of GLUT-1 and GLUT-3 mRNAs was up-regulated under hypoxic conditions [21].

Most striking observation of this experiment was that many interferon-inducible genes were up-regulated in the placenta of TCDD-treated animals. As shown in Fig. 2, 15 out of 18 interferon-inducible genes examined were induced by the TCDD treatment, which strongly suggests that interferon signaling pathway

[22] was activated by the TCDD treatment. We also examined the expression levels of interferon-alpha, -beta, and -gamma by the real-time PCR analysis. Only interferon-beta gene expression was detected, and the level was strongly up-regulated by the TCDD treatment. Although the data suggest that interferon-beta is the key factor, we must take into consideration of the fact that the interferon signaling pathway is activated by many other signaling molecules [23]. The typical interferon signaling pathway is activated through the JAK-STAT system [22]. It is well known that pituitary hormone GH and prolactin also activate the JAK-STAT system [23], and that several prolactin-like molecules including placental lactogen are abundantly produced in the placenta [24]. We can not exclude the possibility that, in addition to interferon-beta, the prolactin-like molecules produced in the placenta may also play significant roles in the induction of interferon-regulated genes.

It is noteworthy that interferon is known to be involved in the regulation of angiogenesis. Interferon-alpha and -gamma were reported to inhibit endothelial cell proliferation [25]. IP-10, one of the interferon-inducible genes, was also strongly induced in the TCDD-treated rat placenta. IP-10 is a member of the alpha-chemokine family, inhibits bone marrow colony formation, has anti-tumor activity *in vivo*, is chemoattractant for monocytes and T cells, and promotes T cell adhesion to endothelial cells. In addition to the above functions, IP-10 has been reported to be a potent inhibitor of angiogenesis *in vivo* [17, 18]. Furthermore, thrombospondin [26] and tissue inhibitor of metalloproteinase 1 (TIMP-1) [27] were also induced by the TCDD treatment, both of which are known to inhibit endothelial cell proliferation. Considering the above observations, the neovascularization in the placenta on GD20 may be impaired by the TCDD treatment through the induction of anti-angiogenic factors.

It is reasonable to speculate that the hypoxic state in the placentas of TCDD-treated rats may be due to the impairment of angiogenesis in the placenta, which may be caused by the activation of the interferon signaling pathway including the production of angiogenesis-inhibitory cytokine IP-10 as well as the production of anti-angiogenic factors such as thrombospondin and TIMP-1.

In conclusion, we identified 81 dioxin-inducible genes and 21 dioxin-suppressive genes from the placenta of TCDD-treated Holtzman rats on GD20. The present study revealed that glucose transporters were strongly up-regulated by the TCDD treatment.

In addition, many interferon-inducible genes were also up-regulated by the TCDD treatment, including IP-10, a potent angiogenesis-inhibitory cytokine. Activation of the interferon signaling pathway and the induction of anti-angiogenic factors may result in the hypoxic state of placenta, which may lead to the increased incidence of fetal death.

## Acknowledgement

The authors thank Yoshiko Inoue for her assistance in manuscript preparation, and T. Nobe for DNA microarray operations. This work was supported in part by grants from the Smoking Research Foundation, Japan Science and Technology Agency, and the Ministry of Health, Welfare and Labour, by 21st Century COE Program (Medical Science), and by the Program for Promotion of Fundamental Studies in Health Sciences of Pharmaceuticals and Medical Devices Agency (PMDA) of Japan.

## References

1. Couture L, Abbott B, Birnbaum L (1990) A critical review of the developmental toxicity and teratogenicity of 2,3,7,8-tetrachlorodibenzo-p-dioxin: recent advances toward understanding the mechanism. *Teratology* 42: 619–627.
2. Birnbaum L (1995) Developmental effects of dioxins and related endocrine disrupting chemicals. *Toxicol Lett* 82–83: 743–750.
3. Lindstrom G, Hooper K, Petreas M, Stephens R, Gilman A (1995) Workshop on perinatal exposure to dioxin-like compounds. I. Summary. *Environ Health Perspect* 103: 135–142.
4. Ohsako S, Miyabara Y, Nishimura N, Kurosawa S, Sakaue M, Ishimura R, Sato M, Takeda K, Aoki Y, Sone H, Tohyama C, Yonemoto J (2001) Maternal exposure to a low dose of 2,3,7,8-tetrachlorodibenzo-p-dioxin (TCDD) suppressed the development of reproductive organs of male rats: dose-dependent increase of mRNA levels of 5alpha-reductase type 2 in contrast to decrease of androgen receptor in the pubertal